Hindawi
Shock and Vibration
Volume 2022, Article ID 5196600, 13 pages
https://doi.org/10.1155/2022/5196600

Research Article

Application of Viscoelastic Tuned Mass Dampers in Vibration Mitigation of Steel Joist Jack Arch Floor Structures

Fatemeh Nikravesh and Hamid Toopchi-Nezhad

Department of Civil Engineering, Razi University, Kermanshah 67149-67346, Iran

Correspondence should be addressed to Hamid Toopchi-Nezhad; toopchi@gmail.com

Received 6 February 2022; Revised 26 April 2022; Accepted 4 May 2022; Published 24 May 2022

Academic Editor: Fabio Botta

A common situation found in many old and modern buildings is the annoying floor vibration. Many old buildings suffer floor vibration as no specific design guidelines were employed to limit the situation. In modern buildings, the development of floors of lighter weight, longer span, and less inherent damping is the main cause for the annoying vibration. In this paper, as a novel application, the influence of viscoelastic tuned mass dampers (TMDs) in vibration mitigation of an existing steel joist jack arch floor structure is investigated using finite element (FE) analysis. Results of a free vibration test conducted on the prototype TMDs are used to validate the FE model. The jack arch floor is subjected to the walking loads of different stepping rates of 1.5, 2, and 3 Hz. Various load models that are available in the literature are used to define the dynamic walking load, and the response mitigation is carried out based on the most critical load models. The influence of design parameters such as the excitation frequency, configuration of the individual dampers in the TMD system, and the mass ratio of the TMD system on the vibration mitigation of the floor structure are investigated in detail. Results of this study indicate that the viscoelastic TMDs are effective in vibration mitigation of jack arch floor structures.

1. Introduction

The annoying vibration due to the human-induced loads including walking and jogging is a major design challenge in many floor structures. Some traditional flooring systems, such as steel joist jack-arch floors, exhibit excess vibrations due to the insufficient flexural rigidity or effective damping of their joists. The annoying vibration can also be found in many modern buildings that employ lightweight construction materials. These buildings typically employ a relatively fewer number of columns as the beams are typically constructed at pretty longer spans and the floor panels become comparatively larger. This may yield to the problem of excessive floor vibrations [1].

The stepping rates for human walking and jogging typically range between 1.5 and 3.2 Hz [2]. In addition, the excitation from human activities also includes higher harmonic components that occur at frequencies larger than the stepping rate. The coincidence of the natural frequency of the floor structure with any of the walking harmonies results in resonant vibrations. The common methods to mitigate the floor vibrations include increasing the natural frequency of the floor structure by improving the bending rigidity of its structural components such as joists and beams and (or) increasing the energy dissipation capability (i.e., effective damping) of the floor system [3]. An increase in the natural frequency alone may not be sufficient to satisfy the vibration serviceability requirements if the floor structure lacks adequate energy dissipation (effective damping) capability [4]. As an alternative approach, tuned mass dampers (TMDs) that vibrate out of phase with the floor vibrations may be employed to counteract the resonant vibrations of the floor structure and dissipate the energy of vibration. TMDs typically offer a cheaper and more practical solution to the vibration mitigation of existing floor structures compared to the other methods such as increasing the flexural rigidity of the floor structure [5]. A TMD device may be idealized as an SDOF mass, spring, and dashpot model. The device operates

effectively over a small frequency range and should be tuned to the frequency of only one of the vibration modes of the structure it is suspended to [6].

The most conventional TMD systems include the attachment of a secondary beam structure [7, 8], which acts as a TMD to the original structural system, and the application of a ball or pendulum type of TMD that is attached to the original system for vibration attenuation [9–11]. In the latter case, the essential points of the design are to find the mass and the radius of the ball or pendulum system [12]. TMDs have been employed in vibration control of different structural and nonstructural systems. These include tall buildings and super high-rise structures [13], high-speed railway bridges [14], pedestrian bridges [15], wind turbines [16], components of mechanical machines [17], etc. The TMDs may be designed as passive [18], semiactive [19, 20], and active motion control devices [21].

The first application of TMDs in floor vibration mitigation was reported by Lenzen back in 1996 when he employed a group of small TMDs with a total mass of about 2% of the effective floor mass to overcome the excessive floor vibrations in a laboratory building [22]. In the said application, the TMDs comprised a 7.5% effective damping ratio, and their frequency tuned 1 Hz lower than the fundamental frequency of the floor structure. Shope and Murray [5] employed fourteen TMDs to mitigate the excessive vibrations in an office floor that had four openings in it. The TMDs were used to control two vibrational modes of the floor system. Saidi et al. [23] evaluated the dynamic characteristics of a prototype viscoelastic TMD and examined the application of the damper in the vibration mitigation of simply supported beams (a steel beam and a reinforced concrete T-beam) through experiments and finite element analysis. Hezarkhani [24] conducted free vibration tests on two prototypes of viscoelastic TMDs to evaluate their dynamic characteristics. Finite element analysis showed the successful application of the TMDs in vibration mitigation of a steel-deck composite floor system. Al-Rumaih and Kashani [25] documented the unsatisfactory performance of a special TMD with viscoelastically damped leaf-spring suspension for vibration mitigation of large floor systems.

In this paper, the application of viscoelastic TMDs in vibration mitigation of an existing steel joist jack arch floor is investigated. The traditional jack arch flooring system was developed in Britain towards the end of the nineteenth century, and later, it became a popular flooring system in parts of East Europe and the Middle East. The advantages of the jack arch system include its simplicity and relatively fast speed of construction, material availability, and relatively low construction cost. Despite these advantages and the widespread application of this flooring system in old buildings, no specific design codes can be found to address its engineering design procedure. This made the jack arch floors be constructed empirically based on previous practices [26]. The jack arch floors typically satisfy the strength requirements in resisting the gravity loads. However, in many cases, including the case study of this paper, they fail to fulfill the vibration serviceability requirements under human-induced dynamic loads such as walking or jogging.

The paper includes the following components. The floor vibration acceptance criteria and different models that simulate the dynamic effects of human walking loads are reviewed. A modal analysis is conducted on a case study of steel joist jack arch floor system to evaluate its modal frequencies and mode shapes using FE analysis. As a novel application for such floor systems, viscoelastic TMDs are designed and implemented to mitigate the floor vibrations. The FE model of the TMDs is verified using the previous experimental data. The influence of various design parameters including the excitation frequency, configuration, and distribution of individual TMDs across the floor panel and the total mass ratio of the TMD system on the floor vibration mitigation are investigated in detail.

1.1. Floor Vibration Criteria. Figure 1 shows the permissible peak acceleration values in a floor system as a function of its natural vibrational frequency. These criteria are proposed by Allen and Murray for the floors of different occupancies including residential, offices, shopping malls, and footbridges. [27]. The ISO [28] baseline curve for the root mean square (RMS) of acceleration is also shown in this figure. These criteria are taken into account in the vibration control of the case studies of this paper.

2. Simulation of Dynamic Effects of Walking

Walking and running cause dynamic loading in the structures. A significant number of studies have been conducted over the past decades to model the dynamic loads due to human activities. The dynamic vertical load, $f_v(t)$ resulting from human walking may be expressed by the following Fourier series [2].

$$f_v(t) = G + G\sum_{i=1}^{n} a_{vi} \sin\left(2i\pi f_p t - \varphi_{vi}\right), \quad (1)$$

where G is the weight of the walking person in Newtons, a_{vi} represents the dynamic magnification factor that depends on the harmonic number i, parameter n reflects the total number of effective harmonies, f_p shows the loading frequency, t is the time variable in seconds, and ϕ_{vi} is the phase delay angle. The number of effective harmonies and the numerical values of f_p, a_{vi}, and ϕ_{vi} for different models are listed in Table 1. By examining this table, it can be seen that a larger share of the applied load is due to the first harmony. Overall, the magnitude of the dynamic load decreases with increasing harmony [2].

A comparison between the time history of the dynamic vertical loads simulated by the various models in Table 1 is shown in Figure 2. The dynamic loads shown in Figure 2 are relevant to the dynamic effects of walking with a frequency of 2 Hz. The frequency of $f_p = 2$ Hz lies within the frequency range of the models cited in Table 1. An examination of Figure 2 indicates that although the general trend of the curves is similar, they differ in detail. This is particularly the case around the local extremum regions of the curves. As such, the response behavior of the floor structure to each load is expected to be different.

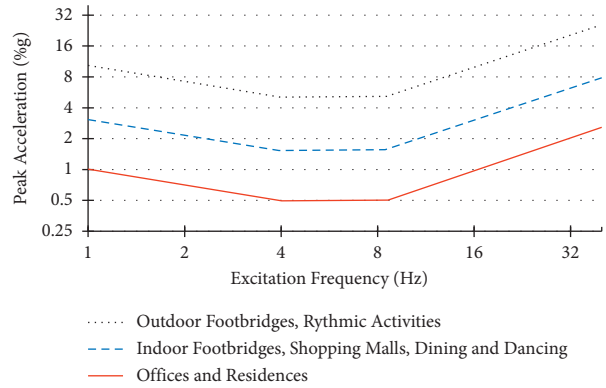

Figure 1: Allen and Murray vibration control criteria [27].

Table 1: Parameter values of various walking load models.

Date	Model	f_p	a_{vi}	Phase angles
1977	Blanchard [29]	—	$a_{v1} = 0.257$	—
1987	Bachmann and Ammann [30]	2.0–2.4	$a_{v1} = 0.4$–0.5, $a_{v2} = a_{v3} = 0.1$	—
1998	Kerr [31]	1–3	$a_{v1} = -0.264 f_p^3 + 1.3206 f_p^2 - 1.7597 f_p + 0.7613$, $a_{v2} = 0.07$, $a_{v3} = 0.06$	—
2001	Young [32]	1–2.8	$a_{v1} = 0.37\ (f_p - 0.95) < 0.56$, $a_{v2} = 0.054 + 0.0044\ f_p$, $a_{v3} = 0.026 + 0.005\ f_p$, $a_{v4} = 0.01 + 0.0051$	—
2011–2012	Chen [33]	1.5–3	$a_{v1} = 0.2817\ f_p - 0.2393$, $a_{v2} = 0.0895$, $a_{v3} = 0.0601$, $a_{v4} = 0.0577$, $a_{v5} = 0.0429$	$\varphi_1 = -\pi/4$, $\varphi_2 = \pi/4$, $\varphi_3 = \pi/2$

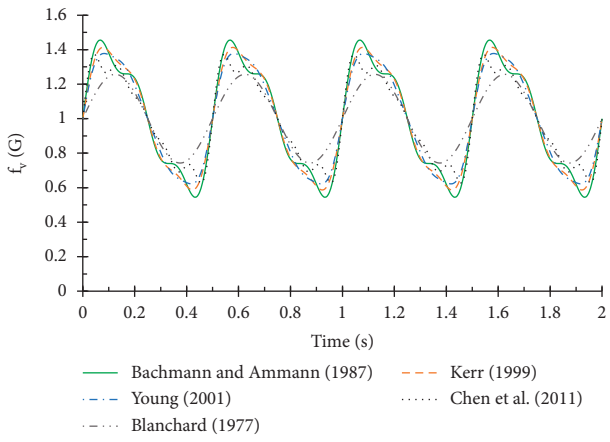

Figure 2: Comparison of various models in the simulation of the walking loads of $f_p = 2$ Hz.

3. Case Study Jack Arch Floor Structure

3.1. Description of the Floor System. The Kermanshah District-3 School Board Building is a 2-story building approximately 40 years old located in Kermanshah, Iran. The floor structure of the building comprises a steel joist jack arch system that employs a series of masonry brick arches supported by steel joists. Figure 3(a) shows the plan view of one of the largest panels of the floor system within the building. The steel joists are simply supported IPE200 with a span of 5.7 m. The joists are supported by the steel beams of IPE220 with a span of 7.2 m.

Figure 3 also includes the cross section of the floor structure. The steel joist jack arch system employs clay brick masonry arches of 0.9 m span to transfer the gravity loads, mainly in compression, to the supporting steel joists. As seen in Figure 3, the top of the masonry brick arch is filled with soil, a layer of portland cement mortar, and eventually, mosaic tiles as the finishing layer. The bottom of the masonry arch is leveled with a leveling plaster that is a mixture of gypsum and soil, and then, a thin layer of gypsum plaster, as the finishing layer, is applied. The total dead load of the floor is estimated to be 4.76 kPa.

The excessive floor vibrations may be decreased by increasing the flexural stiffness of the steel joists and if required the rigidity of their supporting beams. Alternatively, or even, in addition, supplemental dampers may be employed to increase the effective damping of the floor system to attenuate its excess vibrations. In this research study, the application of passive viscoelastic TMDs as a means of vibration attenuation has been investigated.

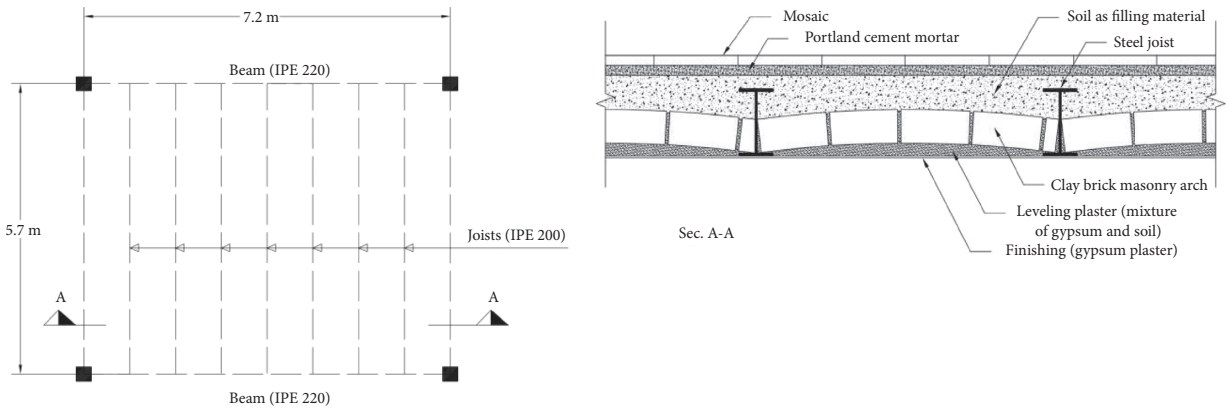

Figure 3: Jack arch flooring system (plan view and the cross section A-A).

3.2. Finite Element Analysis of the Jack Arch Floor. In this study, the dynamic response of the floor structure to the human walking loads is evaluated using a 3D finite element model (FEM) developed in Abaqus [34], a commercial FE-analysis software package. In the FEM, the structural components of the floor system, namely, masonry arches, steel joists, and steel beams, are all defined as individual parts. The parts are then assembled to form the structural system of the entire floor panel. The geometry of the arch, joist, and the beam part is defined in terms of mm in the model. The parts are discretized into finite elements using the C3D8R element type which is a first-order, 3D, 8-node linear brick, reduced integration with hourglass control finite element. Since this element type has only one integration point, it may distort in such a way that the strain values calculated at the integration point remain all zero. This leads to uncontrolled distortion of the element that represents a nonphysical mode of deformation (also termed as hourglass mode). First-order, reduced-integration elements in Abaqus include hourglass control, which attempts to minimize the hourglass mode without inserting excessive constraints on the physical distortion of the element [34].

To define the boundary conditions, the translational degrees of freedom of the finite element nodes located on the web and the bottom flange of the beams were all restrained. Additionally, since the steel joists were simply supported, only the translational degrees of freedom of the nodes located on the web of the joists were restrained.

As the floor structure remains elastic during the vertical vibrations induced by human activities, both the steel and masonry materials are defined as linear elastic. The modulus of elasticity of 2.1e11 Pa is assumed for the steel material, and the value of 2255 Pa is adopted for the masonry material. The joist and arch parts are tied to one another at their physical boundaries using the tie element available in the software program.

Figure 4 shows the first four mode shapes of the floor structure and their natural frequencies evaluated by the FE analysis. An examination of this figure indicates that the frequency of the first two vibrational modes of the floor structure lies within the range of 4 to 8 Hz where the human walking would produce significant vibrations [3]. Thus, this observation justifies the excessive vibrations of the floor structure under human-induced loads.

As it was physically experienced in real practice, a walk-in-place resonance type of loading when applied at the center of the panel resulted in the most annoying vibrations in the floor structure. As such, for simplicity, this study only focused on this type of loading. The investigation of the influence of the other types of loading such as multiple scattered human-induced loads on the floor structure is beyond the scope of the current study and is left for future complementary studies. Accordingly, to evaluate the dynamic response of the floor structure, the point of application of the walking load was placed in the center of the floor panel where the largest vertical deflections would occur. This loading resembles a walk-in-place activity which causes the worst-case scenario with the highest dynamic response in the floor structure. In the FE-analysis runs of this study, the dynamic walk-in-place load as a point load is applied on the middle of the fifth joists of the floor panel, and the response parameters are evaluated at that point. At each analysis run, one of the load models cited in Table 1 is employed to define the dynamic walk-in-place load. The damper design is finalized based on the most demanding load model.

The peak response acceleration values evaluated at the point of application of the walk-in-place load for the various loading models in Table 1 are given in Table 2. The values shown in Table 2 are the FEA output for the walking loads of different load frequencies, f_p, of 1.5, 2, and 3 Hz. Given the vibrational frequency of the first mode, i.e., 5.49 Hz, with the aid of Figure 1, the tolerable peak acceleration limit (i.e., comfort threshold) in the residential and office buildings is evaluated to be 0.05 m/s^2. According to Table 2, the magnitude of the peak acceleration in all cases exceeds this limit which indicates that the vibrations induced by the walk-in-place activity are beyond the threshold of human comfort. As such, the floor system needs vibration attenuation. The viscoelastic tuned mass dampers (TMDs) designed for this reason are described in the next section.

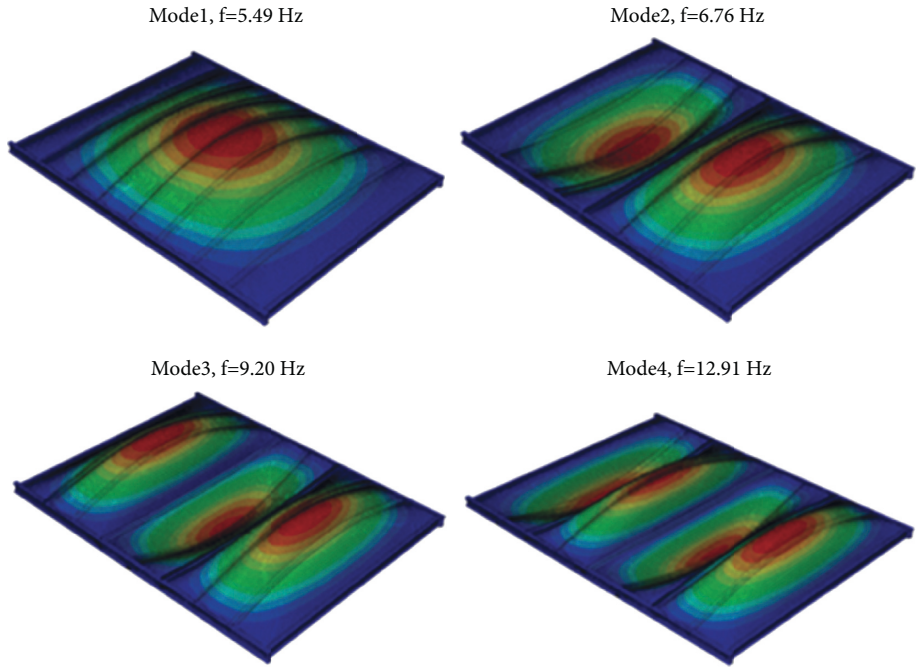

Figure 4: Mode shape analysis of the floor panel (the first four initial vibration modes).

Table 2: Peak response acceleration of the jack arch floor structure under different walk-in-place load models.

Model	Load frequency (Hz)	Peak response acceleration (%g)
Blanchard et al. [29]	1.5	0.086
	2.0	0.029
	3.0	0.076
Bachmann and Ammann [30]	1.5	N/A*
	2.0	0.142
	3.0	N/A*
Kerr [31]	1.5	0.060
	2.0	0.091
	3.0	0.388
Young [32]	1.5	0.078
	2.0	0.074
	3.0	N/A*
Chen [33]	1.5	0.110
	2.0	0.147
	3.0	0.340

*Not applicable as the loading frequency is beyond the valid range of the model.

4. Vibration Attenuation of the Floor Structure

As described in the previous section, the floor structure of this study fails to fulfill the vibrational serviceability requirements under the application of human walk-in-place loads generated by the load models given in Table 2. In this section, the application of viscoelastic tuned mass dampers (TMDs) in vibration mitigation of the floor structure is investigated. The section includes an introduction to the damper device, the FEM of the device, calibration of the FEM based on the available experimental data, the design of viscoelastic TMDs for the floor structure, and finally the response evaluation of the floor structure that is equipped with viscoelastic TMDs.

4.1. Viscoelastic TMDs. The tuned mass damper (TMD) of this study includes a composite cantilever arm that supports a concentrated mass at its end (see Figure 5). The cross section of the cantilever arm comprises an inner layer of viscoelastic material which is bonded to two outer steel plates. The self-weight of the cantilever arm is typically negligible as compared to the weight of the solid mass connected at its end. Thus, the magnitude of the solid mass may be assumed with sufficient accuracy as the effective mass of the TMD system. The stiffness of the TMD system arises from the flexural stiffness of the cantilever arm. This stiffness is affected by the arm length and its cross-sectional dimensions. The effective damping of the TMD system is related to the inherent damping of its inner viscoelastic layer. The contribution of the steel plates in damping is minimal as these plates remain elastic during the operation of the damper.

The TMD is activated with the vibrations of the original floor structure. The back-and-forth flexural deformations in the damper arm result in energy dissipation due to the reversal shear deformations in the inner viscoelastic layer. The effective damping of the TMD system stems from the inherent damping of its viscoelastic material. The effective damping of the TMD is also affected by the physical volume of the viscoelastic material employed in the cantilever arm of the damper. A filled compound of neoprene rubber was employed as the viscoelastic material. Figure 6 shows a typical application of the viscoelastic TMD in vibration mitigation of the steel joists of the jack arch floor system. As seen in this figure, the damper is connected to the bottom

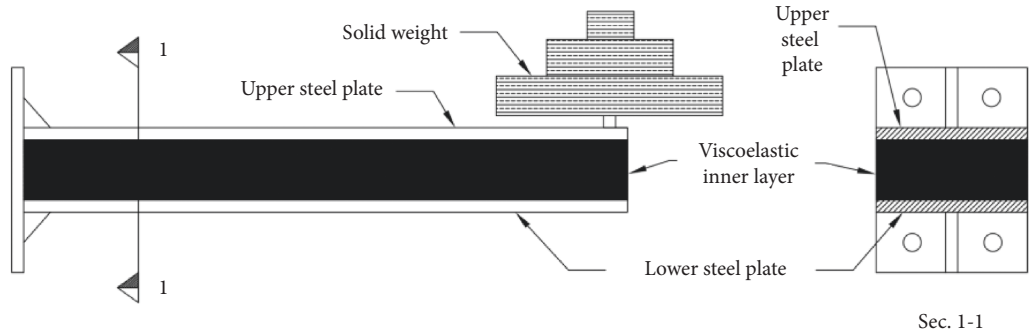

Figure 5: Schematic diagram of a viscoelastic tuned mass damper.

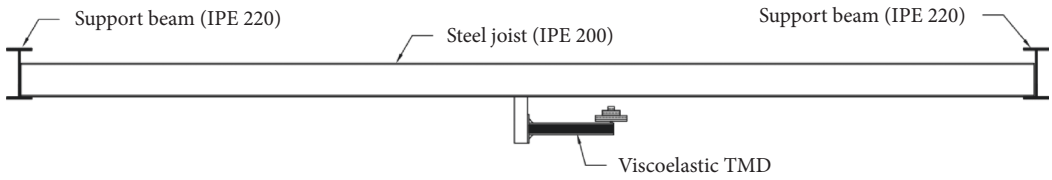

Figure 6: Typical Installation of the TMD to the steel joist (side view).

flange of the steel joist with its arm running parallel to the joist. This damping configuration was found to be the most effective one in the response attenuation of the vibrating joists [1].

Each TMD forms a single degree of freedom structural system that may be idealized by a mass, spring, and dashpot. To be most effective in response attenuation, the vibrational frequency of the TMD should be tuned to match one of the fundamental natural frequencies of the original structure. The frequency of the viscoelastic TMD of this study may be tuned by changing the magnitude of the concentrated mass, the effective length of the cantilever arm of the damper, and/or its cross-sectional dimensions. The mass ratio which represents the ratio of the damper to structural mass plays an important role in the performance of a TMD. Given the practical limitations, the use of a mass ratio of 1% to 5% is common in the cost-effective application of TMDs.

The FEM of the viscoelastic TMDs of this study was calibrated using the results of a previous experimental study conducted by Hezarkhani [24]. Table 3 includes the geometrical characteristics of the prototype viscoelastic TMD. Figure 7 shows the test setup employed to evaluate the dynamic characteristics of the prototype damper using a set of free vibration tests. A linear variable differential transducer (LVDT) that is attached to the tip of the cantilever arm of the TMD measures the vertical deflections. The free vibration of the damper under different initial displacements of 10 to 15 mm is monitored with an LVDT and recorded with a dynamic data logger. The fundamental frequency and equivalent viscous damping ratio of the damper are evaluated to be 5.8 Hz and 4.8%, respectively, from the free vibration tests [24]. The free vibration tests which are initiated from an at-rest condition are performed under various initial deflections that bracket the deflections expected in the damper device during its operation. Since the free vibration tests are adjusted over the operational range of deflections of the device, no significant variations in the effective stiffness and acting frequency of the device with its experimentally evaluated values are expected during its operation in vibration mitigation of the floor structure.

Table 3: Geometric specifications of the prototype damper tested in Ref. [24].

Damper arm length (L)	580 mm
Damper arm width (b)	100 mm
Thickness of steel plates (t_s)	6 mm
Thickness of viscoelastic layer (t_r)	420 mm
Mass (m)	28 kg

Figure 7: Free vibration test on the prototype viscoelastic TMD [24].

To validate the numerical modeling of the damper device, the free vibration tests conducted on the prototype damper by Ref. [24] are simulated with the aid of FE analysis. The components of the damper arm, including the upper and lower steel plates and the inner elastomeric layer, are defined as individual parts in the Abaqus model. The C3D8R finite

elements available in Abaqus/Standard [34] are utilized to mesh the steel parts. The inner viscoelastic elastomeric layer of the damper arm is discretized using the C3D8H element type, which is a linear hexahedral hybrid element with constant pressure. Hybrid elements are available in Abaqus/Standard for the FE formulation of incompressible materials. The hyperelastic behavior of the elastomeric material is simulated by fitting the Marlow Model to the experimental uniaxial stress-strain curve of the elastomer material (shown in Figure 8), and the viscoelastic behavior is modeled with the Prony Series [34]. Abaqus employs a Prony series expansion of the dimensionless relaxation modulus, 4, to model the viscoelastic material behavior. The one-term version of the Prony series may be written as in the following equation [34]:

$$g_R(t) = 1 - g\left(1 - e^{-t/\tau}\right), \tag{2}$$

where g and τ are material constants. A similar Prony series expansion is used for the volumetric response. The one-term version of the said series is given in the following equation [34]:

$$p = -K_0\left(\varepsilon^{\text{vol}} - \frac{k}{\tau}\int_0^t e^{-s/\tau}\varepsilon^{\text{vol}}(t-s)ds\right). \tag{3}$$

The parameters g, k, and τ which can be defined directly in the Prony series are evaluated from the calibration of the model to the available free vibration test data on the damper device. Since the relaxation time is associated with the relaxation modulus only, a zero value has been assigned to parameter k as recommended by the Abaqus analysis manual. The numerical values of the model coefficients employed in the FE analysis for the steel and elastomeric materials are given in Table 4.

The parts defined for the outer steel plates and the inner elastomeric layer are assembled to form the composite arm of the damper. The parts are tied to one another at their contact boundaries using the tie elements available in Abaqus/Standard [34]. The concentrated mass of 28 kg at the end of the damper cantilever arm (see Figure 7) is defined as a lumped mass in the FEM.

Figure 9 shows the first vibrational mode shape of the damper device evaluated by the FEM. The natural frequency obtained by the FEM is 5.81 Hz, which is in excellent agreement with the experimental value reported in Ref. [24]. This verifies the accuracy of the FEM in evaluating the mode shapes of the viscoelastic TMDs of this study.

To simulate the response history during the free vibration test, the FE analysis is conducted in two steps. First, a displacement of 15 mm is applied to the end of the damper arm in a displacement control static analysis. Then, as the next step of the analysis, the initial displacement is released in a free vibration dynamic analysis. Figure 10 includes the free vibration time history plots of the damper evaluated by the FE analysis (current paper) and the experimental study (Ref. [24]). The displacements shown in Figure 10 reflect the vertical deflections at the end of the damper arm where the lumped mass is located. A close examination of Figure 10

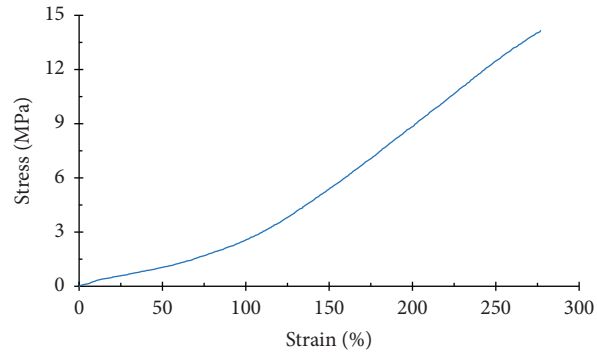

Figure 8: Uniaxial stress-strain behavior of the viscoelastic material [24].

Table 4: Mechanical properties of the materials of the damper device.

Energy dissipation factor (β)	0.12
Shear modulus of viscoelastic material (G_e)	0.650 MPa
Poisson's ratio of steel (υ_s)	0.30
Modulus of elasticity of steel (E_s)	210 GPa
Poisson's ratio of viscoelastic material	0.49
Prony series material constants g, k, τ	0.98, 0, 0.0055

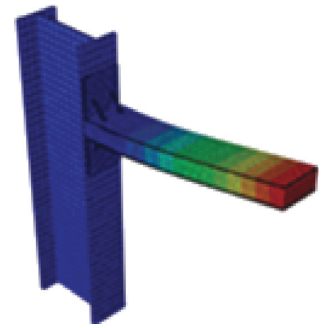

Figure 9: Fundamental mode shape of the prototype viscoelastic damper evaluated by the FEM.

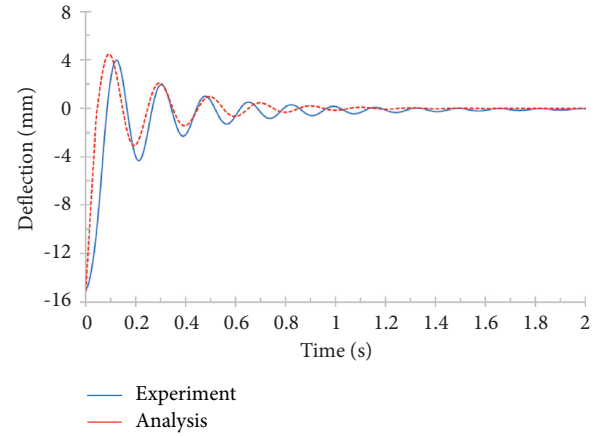

Figure 10: Free vibration response history of the prototype TMD (analysis vs. experimental results).

indicates that during the first few cycles of vibration, there is a good correlation, with a maximum error of 11%, between the FEM and experimentally recorded data. At the lower displacement amplitudes, however, the model vibrations seem to be attenuated at a relatively higher rate as compared to the experimental observations.

4.2. Application of TMDs in Floor Vibration Attenuation. To mitigate the vibrations of the jack arch floor shown in Figure 4, two different viscoelastic TMDs, namely, TMD Types 1 and 2, are designed. The fundamental vibrational frequency of both damper Types 1 and 2 are evaluated to be 5.49 Hz from the FEA, which resembles a perfect match with the frequency of the floor structure. In TMD Type 1, the damper length is designed to be 650 mm, and its mass is taken as 13.50 kg. The TMD Type 2 employs an arm length of 550 mm with a lumped mass of 18.45 kg. The two TMD types are concordant as they are perfectly tuned at the fundamental frequency of the floor structure. This harmony permits their concurrent application in a damper group that is designed for vibration mitigation of the floor structure. The combined application of the TMD types in the floor structure will provide further flexibility in achieving different mass ratios in the TMD group. The specifications of the two designed TMD types are shown in Table 5.

As the joists of the floor structure are simply supported, only half of the floor mass, i.e., 8 tons, is effective in its dynamic vibrations [1]. Different combinations of the viscoelastic TMDs with total mass ratios of approximately 1%, 2%, and 3% are investigated in this section. The TMDs in each case are attached to the steel joists of the floor system. Moreover, in all cases, the damper arm is oriented along the length of the joist, as seen in Figure 6. To achieve a total mass ratio of 1% in the TMD system, a group of 8 TMDs of Type 1, each with a concentrated mass of 13.5 kg, is utilized in three different arrangements shown in the reverse plan view (view from the bottom of the floor) in Figure 11. Among the three arrangements shown in this figure, the first arrangement (Arrangement A), based on the analysis results, is found to be more effective in vibration mitigation of the floor system. In this arrangement, all of the steel joists of the floor structure enjoy at least one TMD device at its midspan, where maximum deflections are expected. Moreover, the middle joist, as the most critical joist of the floor with the largest deflection (see the mode shapes shown in Figure 4), employs two TMDs in the vicinity of its midspan.

To achieve TMD systems of 2% and 3% mass ratio, the arrangements shown in Figures 12(a) and 12(b) that employ Type 2 of the TMDs are found to be most effective in the vibration attenuation of the floor system. In these arrangements, all of the steel joists are equipped with dampers. The dampers are most effective in vibration mitigation when installed at locations with maximum deflection. The effective distribution of dampers among the joists is the one that is the most consistent with the deflected surface of the floor structure in its dominant mode of vibration (see Figure 4).

To assess the performance of the TMDs in vibration mitigation of the floor structure, the time history of vertical accelerations induced at the center of the floor panel is evaluated. The center of the panel is located at the middle length of the 5th steel joist. Figure 13 shows the response acceleration history of the said point under the walk-in-place loading generated by the Young Model with an input frequency of 2 Hz before and after installation of the TMD system having 3% effective mass. As seen, the TMD system significantly decreases the peak response accelerations in the floor system. The peak acceleration of the original floor decreased from 0.074 m/s^2 (7.54 mg) to 0.017 m/s^2 (1.73 mg) after the installation of the viscoelastic dampers. This corresponds to 77% response mitigation.

Table 5: Specifications of the viscoelastic TMDs.

Property	Type 1	Type 2
Arm length (L)	650 mm	550 mm
Arm width (b)	100 mm	100 mm
Thickness of the outer steel plates (ts)	4 mm	4 mm
Thickness of the inner elastomeric layer (tr)	42 mm	42 mm
Energy dissipation factor (β)	0.12	0.12
Shear modulus of viscoelastic material (G)	0.65 MPa	0.65 MPa
Lumped mass ($m_{n\,d}$)	13.5 kg	18.45 g
Natural frequency (f_2)	5.49 HZ	5.49 HZ

To assess the vibration serviceability requirements, it is critical to evaluate the magnitude of the peak response acceleration that is experienced by the floor structure under the application of walking load. As such, Figure 14 includes the peak acceleration values before and after the installation of the TMDs. The vertical axes in Figure 14 represent the absolute peak acceleration response in terms of m/s^2 evaluated at the center of the floor panel. The maximum weight of 700 N is assumed for the walking person in all of the load models that are investigated in this paper. As seen in Figure 14, there is a significant difference between the peak acceleration values resulting from different loading models. Among the load models investigated in this paper, the model proposed by Chen et al. [2] provides the largest dynamic effects in the original floor structure at load frequencies of 1.5 and 2 Hz. Nonetheless, the largest peak acceleration induced in the original floor structure under the loading frequency of 3 Hz belongs to the load model developed by Kerr [31]. The red horizontal dashed lines in Figure 14 indicate the maximum tolerated floor acceleration for the office buildings in conformance with Allen and Murray's acceptance criteria [3]. As seen in Figure 14, the peak accelerations in the original floor system under loading frequencies of 1.5 to 3 Hz rise beyond the level of comfort threshold regardless of the load model employed in the analysis. The influence of the TMD mass ratio on mitigating the floor vibrations under various excitation frequencies of 1.5, 2, and 3 Hz may be assessed by the inspection of Figure 14. A close examination of the chart bars in Figure 14 indicates that irrespective of the magnitude of the excitation frequency and the load model used, the peak acceleration is decreased with increasing TMD mass ratio.

At the loading frequency of 1.5 Hz, the application of the TMDs of 1%, 2%, and 3% mass ratios result in 29%, 55%, and 59% floor vibration attenuation, respectively, when the walk-

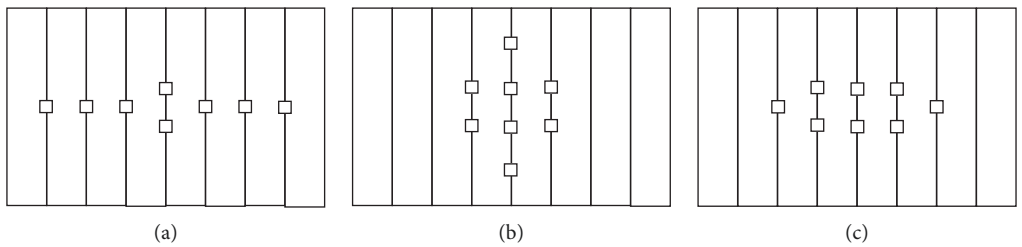

Figure 11: Different arrangements of dampers in a TMD system of 1% mass ratio (reverse plan view).

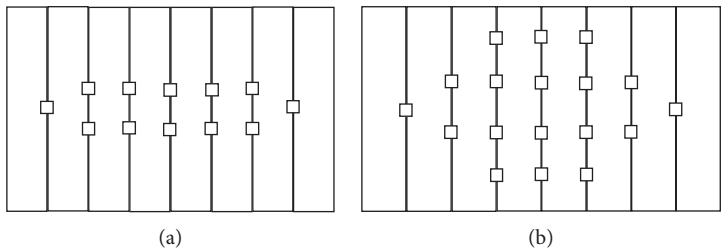

Figure 12: Optimal damper arrangement (reverse plan view) in the TMD systems of (a) 2% mass ratio and (b) 3% mass ratio.

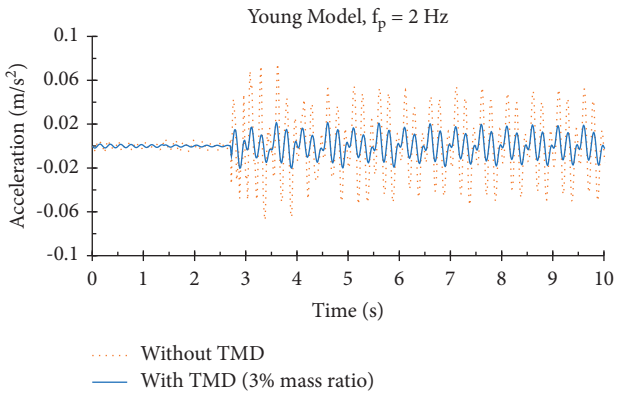

Figure 13: Typical history plots of the floor acceleration before and after the installation of TMDs.

in-place load is simulated by Chen et al.'s Model [2]. The 2% mass ratio is enough to satisfy the vibration serviceability requirements for the loading frequency of 1.5 Hz. At the loading frequency of 2 Hz, the level of response mitigations achieved in the floor system using the Chen et al.'s Model [2] is 57%, 79%, and 81% for the TMDs of 1%, 2%, and 3% mass ratios, respectively. Again, the 2% mass ratio in the TMD system is sufficient to decrease the peak floor accelerations down to the level of comfort threshold.

The 3 Hz loading frequency is more critical as it results in the largest peak acceleration in the floor system. The original floor system is most influenced by the 3 Hz Kerr load model [31], where the peak acceleration at the center of the floor structure reaches 0.38 m/s^2. The 2% mass ratio in the TMD system, using the Kerr Model [31], is sufficient to limit the floor peak acceleration to its permissible value. On the contrary, when the Chen Model [33] is used to simulate the dynamic effects of the walk-in-place loading of 3 Hz, application of the TMD of 2% mass ratio although results in a significant 75% response attenuation and fails to sufficiently mitigate the floor vibrations. Application of the TMD of 3% mass ratio results in 88% response reduction in the floor system under the 3 Hz Chen Model [33] which is sufficient to satisfy the floor vibration serviceability requirement.

As seen in Figure 14, in general, a TMD mass ratio of 2% is sufficient to decrease the peak-induced floor accelerations to the permissible limit in all cases, but the 3 Hz Chen Model [33]. However, at this rate of loading, the induced floor vibrations can well be mitigated by a TMD system of a 2% mass ratio when the Kerr Model [31] is employed in the analysis. The discrepancy between the optimistic results of the Kerr Model and the pessimistic results of the Chen et al.'s Model can best be judged by the experimental evaluation of the floor response equipped with the TMD system of 2% mass ratio under 3 Hz walk-in-place loads. In the absence of such experimental data, one may conservatively employ the TMD system of a 3% mass ratio to limit the floor vibrations with a larger safety margin.

Figure 15 shows the profiles of the peak accelerations along the width of the floor panel when equipped with the TMD systems of different mass ratios. The acceleration values shown in this figure are evaluated at the middle length of the steel joists of the floor system when the walk-in-place loads of different loading frequencies of 1.5, 2, and 3 Hz are applied at the center of the floor panel right on the middle length of the central joist #5. The walk-in-place load is simulated using the Chen [33] Model as the most demanding model in comparison with the other models studied in this paper.

As expected, the peak accelerations are diminished with increasing distance from the point of application of the dynamic load (i.e., the center of the floor panel). An examination of Figure 15 indicates that the performance of the TMDs of 2% and 3% mass ratio is approximately the same along the width of the floor for the loading frequencies of 1.5 and 2 Hz. At the higher rate of loading, i.e., load frequency of

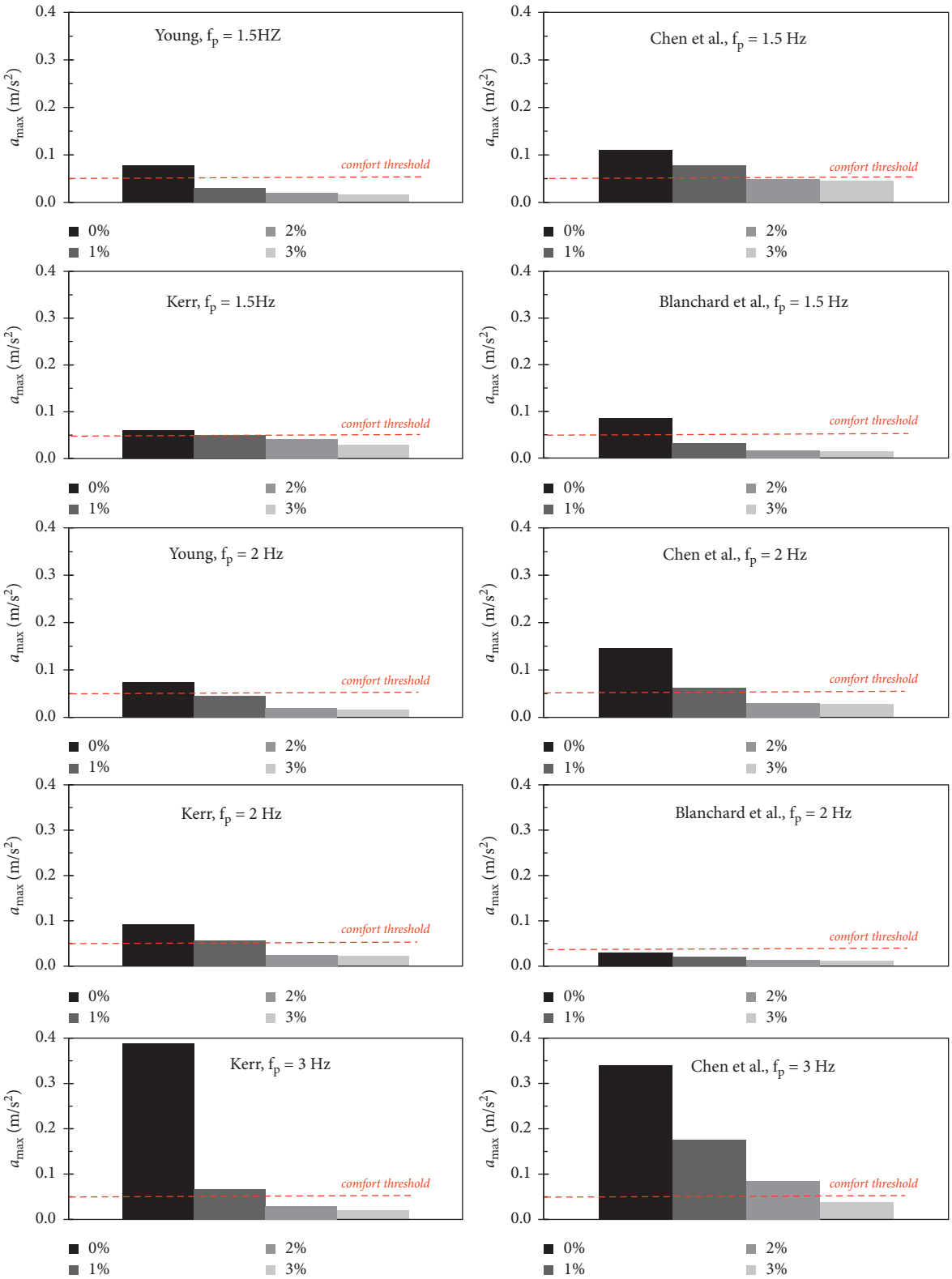

Figure 14: The peak acceleration of the floor structure equipped with the TMD systems of different mass ratios under different walk-in-place load models and frequencies.

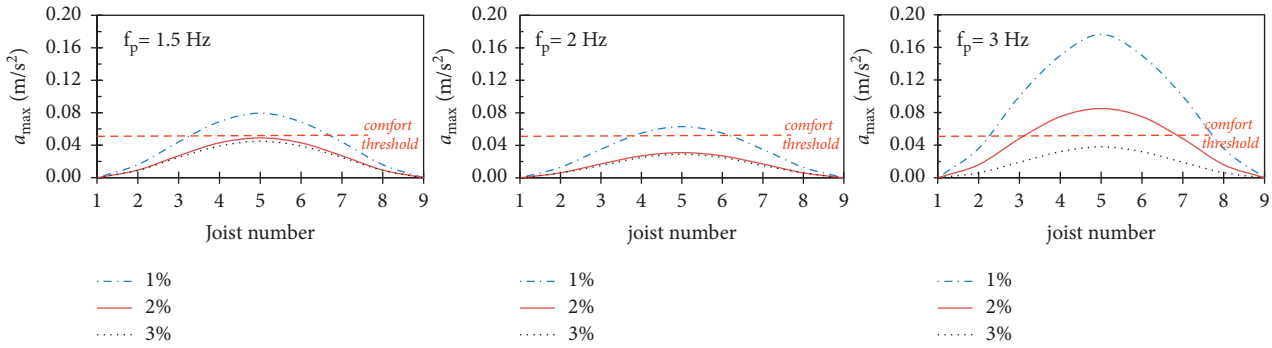

Figure 15: Profiles of the peak response acceleration evaluated along the width of the floor structure equipped with the TMDs of different mass ratios, μ, of 1% to 3% under various excitation frequencies.

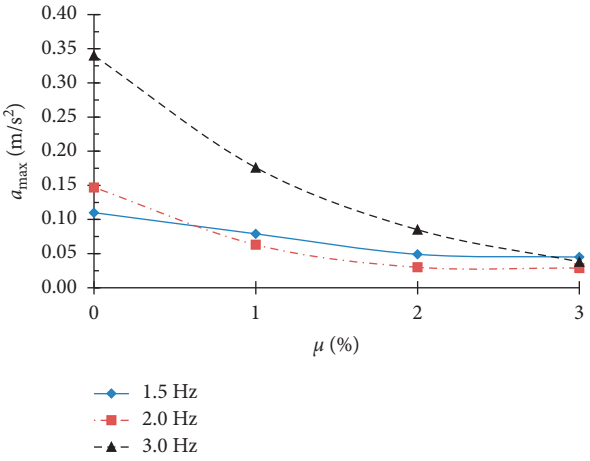

Figure 16: Variations of the peak floor acceleration with the TMD mass ratio for loads of different frequencies.

3 Hz, the induced accelerations at a significant portion of the floor at its central region stay above the threshold limit. The use of a 3% mass ratio in the TMD system successfully controls the annoying vibrations of the floor structure.

The influence of the TMD mass ratio, μ, on the floor peak response acceleration under the walk-in-place loads of different frequencies is shown in Figure 16. The dynamic effects of loading in Figure 16 are simulated by Chen [33] Model. As seen in this figure, the rate of decrease in the peak acceleration with increasing mass ratio is not the same for loads of different frequencies. The higher the frequency of the load is, the more sensitive to the TMD mass ratio the floor response is.

It should be noted that in addition to the mass ratio, the performance of TMDs depends on the distribution of the masses throughout the floor structure. Figure 16 which indicates the influence of mass ratio on the vibration mitigation performance of the TMD system is valid for the mass distributions studied in this paper.

As seen in Table 5, two TMD design types are investigated in this study. The total mass of the TMD Types 1 and 2 is 20.3 kg and 24.2 kg, respectively. In the worst-case scenario, the maximum vertical deflection of the steel joist as a result of the installment of four TMDs on it is calculated to be 0.72 mm. This is approximately 11% of the joist deflection under the design live load of 2 kPa. The peak vertical deflection in the steel joist when it supports two TMDs is 0.45 mm (i.e., nearly 7% of the joist deflection under its design live load). In a TMD arrangement similar to the one that is given in Figure 12(b) when the two adjacent joists support different numbers of TMDs, the maximum differential deflection between the joists is expected to be approximately 0.27 mm which is only 0.03% of the span of the masonry arch. As such, the influence of this insignificant differential deflection on the stability and load-bearing resistance of the masonry arch may be neglected.

5. Conclusions

In this paper, the application of novel viscoelastic tuned mass dampers (TMDs) in vibration mitigation of a jack arch floor structure under walk-in-place loads with different frequencies of 1.5, 2, and 3 Hz was investigated. The viscoelastic TMD comprised a composite cantilever arm supporting a concentric mass at its end. The cross section of the cantilever arm included two outer steel plates that were bonded to an inner viscoelastic layer. The finite element model (FEM) of the viscoelastic TMD was calibrated using previous experimental free vibration tests conducted on their prototypes. Using the FEM, two design alternatives for the viscoelastic TMDs having different arm lengths and mass magnitudes were presented. The designed TMDs had the same vibrational frequency that matched the 5.8 Hz fundamental frequency of the floor structure. The influence of the TMD systems of different mass ratios of 1%, 2%, and 3% on vibration mitigation of the floor structure was studied via FEA. The main outcomes of this study are as follows.

(1) The viscoelastic TMDs of this paper were found to be effective in vibration attenuation of the jack arch floor structure.

(2) The level of vibration mitigation achieved is increased with increasing TMD mass ratio. The peak response acceleration was mitigated by 50% when the floor was equipped with a viscoelastic TMD system of a 1% mass ratio. The TMD mass ratios of 2% and 3% resulted in 80% and 94% response mitigation, respectively.

(3) The rate of decrease in the floor peak acceleration with increased TMD mass ratio is affected by the magnitude of loading frequency. The floor response is more sensitive to the TMD mass ratio when the loads are of higher frequencies.

(4) A viscoelastic TMD mass ratio of 2% is sufficient to successfully mitigate the vibrations of the jack-arch floor of this study.

Data Availability

Data will be available by the corresponding author on request.

Conflicts of Interest

The authors have no conflicts of interest to declare regarding the publication of this paper.

References

[1] F. Nikravesh, "Application of viscoelastic mass dampers in vibration mitigation of a structural floor system: a case study. M.Sc. Thesis," in *The Department of Civil Engineering*Razi University, Kermanshah, Iran, 2021.

[2] J. Chen, Z. Han, and R. Xu, "Effects of human-induced load models on tuned mass damper in reducing floor vibration," *Advances in Structural Engineering*, vol. 22, no. 11, pp. 2449–2463, 2019.

[3] T. M. Murray, D. E. Allen, and E. E. Unger, *Steel Design Guide Series 11: Floor Vibrations Due to Human Activity*, American Institute of Steel Construction (AISC), Chicago, 1997.

[4] N. Haritos, E. Gad, and J. Wilson, *Evaluating the Dynamic Characteristics of Floor Systems Using Dynamic Testing*, pp. 225–230, Proceedings of ACAM2005, Melbourne, Australia, 2005.

[5] R. L. Shope and T. M. Murray, "Using tuned mass dampers to eliminate annoying floor vibrations," in *Restructuring: America and beyond*ASCE, 1995.

[6] J. Den Hartog, *Mechanical Vibrations*, pp. 122–169, McGraw-Hill Book Company, New York, 1956.

[7] T. Aida, K. Kawazoe, and S. Toda, *Vibration Control of Plates by Plate-type Dynamic Vibration Absorbers*, 1995.

[8] D. J. Thompson, "A continuous damped vibration absorber to reduce broad-band wave propagation in beams," *Journal of Sound and Vibration*, vol. 311, no. 3-5, pp. 824–842, 2008.

[9] M. Pirner, "Actual behaviour of a ball vibration absorber," *Journal of Wind Engineering and Industrial Aerodynamics*, vol. 90, no. 8, pp. 987–1005, 2002.

[10] E. Matta and A. De Stefano, "Robust design of mass-uncertain rolling-pendulum TMDs for the seismic protection of buildings," *Mechanical Systems and Signal Processing*, vol. 23, no. 1, pp. 127–147, 2009.

[11] R. R. Gerges and B. J. Vickery, "Design of tuned mass dampers incorporating wire rope springs: Part II: simple design method," *Engineering Structures*, vol. 27, no. 5, pp. 662–674, 2005.

[12] F. Yang, R. Sedaghati, and E. Esmailzadeh, "Vibration suppression of structures using tuned mass damper technology: a state-of-the-art review," *Journal of Vibration and Control*, vol. 28, no. 7-8, pp. 812–836, 2021.

[13] Z. Lu and H. B. X. Zhang, "Shaking table test and numerical simulation on vibration control effects of TMD with different mass ratios on a super high-rise structure," *The Structural Design of Tall and Special Buildings*, vol. 27, no. 9, Article ID e1470, 2018.

[14] J. F. Wang, C. C. Lin, and B. L. Chen, "Vibration suppression for high-speed railway bridges using tuned mass dampers," *International Journal of Solids and Structures*, vol. 40, no. 2, pp. 465–491, 2003.

[15] W. Shi and L. Z. Q. Wang, "Application of an artificial fish swarm algorithm in an optimum tuned mass damper design for a pedestrian bridge," *Applied Sciences*, vol. 8, no. 2, p. 175, 2018.

[16] B. Zhao and H. Z. Z. Gao, "Shaking table test on vibration control effects of a monopile offshore wind turbine with a tuned mass damper," *Wind Energy*, vol. 21, no. 12, pp. 1309–1328, 2018.

[17] N. D. Sims, "Vibration absorbers for chatter suppression: a new analytical tuning methodology," *Journal of Sound and Vibration*, vol. 301, no. 3-5, pp. 592–607, 2007.

[18] C. C. Lin and C. M. J. F. R. Y. Hu, "Vibration control effectiveness of passive tuned mass dampers," *Journal of the Chinese Institute of Engineers*, vol. 17, no. 3, pp. 367–376, 1994.

[19] W. Shi and L. Z. H. Wang, "Experimental and numerical study on adaptive-passive variable mass tuned mass damper," *Journal of Sound and Vibration*, vol. 452, pp. 97–111, 2019.

[20] D. Hrovat, P. Barak, and M. Rabins, "Semi-active versus passive or active tuned mass dampers for structural control," *Journal of Engineering Mechanics*, vol. 109, no. 3, pp. 691–705, 1983.

[21] J. C. H. Chang and T. T. Soong, "Structural control using active tuned mass dampers," *Journal of the Engineering Mechanics Division*, vol. 106, no. 6, pp. 1091–1098, 1980.

[22] K. H. Lenzen, "Vibration of steel joist-concrete slab floors," *AISC. Eng. Jour.*vol. 3, pp. 133–136, 1966.

[23] I. Saidi and E. F. J. L. N. Gad, "Development of passive viscoelastic damper to attenuate excessive floor vibrations," *Engineering Structures*, vol. 33, no. 12, pp. 3317–3328, 2011.

[24] H. Hezarkhani, *The performance of viscoelastic tuned mass dampers. M.Sc. Thesis The Department of Civil Engineering*Razi University, Kermanshah, Iran, 2018.

[25] W. S. Al-Rumaih and A. R. Kashani, "A viscoelastic tuned mass damper for vibration treatment of large structures," in *ASME International Mechanical Engineering Congress and Exposition*American Society of Mechanical Engineers (ASME), 2021.

[26] M. R. Maheri and H. Rahmani, "Static and seismic design of one-way and two-way jack arch masonry slabs," *Engineering Structures*, vol. 25, no. 13, pp. 1639–1654, 2003.

[27] A. Ebrahimpour and R. L. Sack, "A review of vibration serviceability criteria for floor structures," *Computers & Structures*, vol. 83, no. 28-30, pp. 2488–2494, 2005.

[28] International Organization for Standardization, *Bases for Design of Structures-Serviceability of Buildings and Walkways against Vibrations*, ISO, 2007.

[29] J. Blanchard, B. Davies, and J. Smith, "Design criteria and analysis for dynamic loading of footbridges," in *Proceedings of the a Symposium on Dynamic Behaviour of Bridges at the Transport and Road Research Laboratory*, Crowthorne, Berkshire, England, May 1977.

[30] H. Bachmann and W. Ammann, *Vibrations in structures: induced by man and machines*, Iabse, vol. 3, , 1987.

[31] S. C. Kerr, *Human Induced Loading on Staircases*, University of London, University, College London (United Kingdom), 1999.
[32] P. Young, "Improved floor vibration prediction methodologies," in *ARUP Vibration Seminar*, vol. 4, 2001.
[33] J. Chen, "Experiments on human-induced excitation using 3D motion capture and analysis," in *Proceedings of the 3rd Asia-Pacific Young Researchers and Graduates Symposium*, Taipei, Taiwan, China, March 2011.
[34] M. Smith, *ABAQUS/Standard User's Manual*, Providence, RI, USA, Dassault Systèmes Simulia Corp, 2009.